



Time-dependent density functional theory calculations of molecular static and dynamic polarizabilities, cauchy coefficients and their anisotropies with atomic numerical basis functions[☆]

Anguang Hu^a, Darrin M. York^{b,1}, Tom K. Woo^{a,*}

^aDepartment of Chemistry, The University of Western Ontario, London, Ont., Canada N6A 5B7

^bDepartment of Chemistry, University of Minnesota, 207 Pleasant St. SE., Minneapolis, MN 55455-0431, USA

Received 15 February 2002; accepted 25 March 2002

Abstract

Static and dynamic polarizabilities of a range of small first row compounds have been calculated with time-dependent density functional theory in the local spin-density approximation using numerical atomic basis sets. The results are compared to earlier computational work, in particular the work of Van Caillie and Amos [C. Van Caillie, R.D. Amos, Chem. Phys. Lett. 291 (1998) 71], as well as experimental values. The results for static isotropic and anisotropic polarizabilities of H₂O, N₂, CO, NH₃, and CH₄ are in good agreement with previous calculations. The results for the dynamic polarizabilities as expressed in the $S(-4)$ Cauchy coefficients and their anisotropies for H₂O, N₂, CO₂, NH₃, CH₄, C₂H₂, C₂H₄ and C₂H₆ are also in good agreement with previous results. We have also explored the scaling of our implementation of the time-dependent coupled-perturbed Kohn–Sham equations by evaluating the static and dynamic polarizabilities of bifurcated water chains ranging from 1–20 molecules in size. © 2002 Elsevier Science B.V. All rights reserved.

Keywords: Molecular polarizabilities; Dynamic polarizability; Time-dependent density functional theory; Numerical basis sets

1. Introduction

Molecular dipole polarizability is a basic and important property that can be used to understand intermolecular forces [1] and the propagation of light through molecules and solids. For example, the frequency dependence of the polarizability can be

used to determine the dielectric constant and the conductivity of materials. Also, the poles in the polarizability at real frequencies give the positions of electronic absorptions and the polarizabilities at imaginary frequencies can be related to the dispersion energy [46].

The calculation of frequency dependent polarizabilities and related properties based on ab initio quantum chemistry is well established for both molecules and periodic systems [2–10]. The calculation of these properties has been extended to correlated electronic structure methods such as Møller–Plesset theory, coupled-cluster theory and recently to density functional theory (DFT) [11–30].

[☆] This paper is dedicated to Professor Bill Meath.

* Corresponding author. Tel.: +1-519-661-2111; fax: +1-519-661-3022.

¹ Corresponding co-author. Tel.: +1-612-624-8042; fax: +1-612-626-7547.

E-mail addresses: twoo@uwo.ca (T.K. Woo), york@chem.umn.edu (D.M. York).

Due to its favorable balance of accuracy and computational expense, DFT has become a widely used method [11,17,20,31,32]. Linear response properties of electronic systems, such as dynamic polarizabilities, can be treated within the time-dependent density functional theory (TDDFT) framework through the coupled Kohn–Sham equations [33, 34]. There are two categories of TDDFT methods [11], one based on the linear response of the electron density and the other based on the linear response of the density matrix of the Kohn–Sham model system. As with traditional correlated electronic structure calculations, the nature of the basis set employed to calculate the response properties with TDDFT is an important issue. Due to the long-range effects of response properties, the use of augmented and diffuse functions in the basis is particularly important [35].

Recently York and co-workers we have developed an efficient implementation of TDDFT for molecular systems using atomic numerical basis functions and a completely numerical approach to solve the Poisson equations required to determine the response density [36]. We use numerical atomic basis sets similar to those developed by Delley [31,37–40]. Compared to commonly used Gaussian basis functions, numerical atomic basis functions have the correct long-range behavior and are therefore expected to be better for determining the dynamic polarizability of molecules and related properties [35]. In this paper, we present calculations on the dynamic polarizability, Cauchy coefficients, and their anisotropies for small first row element compounds with TDDFT in the local spin-density approximation (LDA) using numerical atomic basis sets. The dynamic polarizabilities are emphasized since they are less commonly reported with DFT. The efficiency and effective scaling of our implementation will be examined by determining the dynamic polarizabilities of water chains.

2. Theoretical and computational details

Static and dynamic polarizabilities have been calculated based on a recent implementation of the time-dependent coupled-perturbed Kohn–Sham equations using atomic numerical basis functions and a completely numerical approach to solve the Poisson equations required to determine the response

density [36]. We will only briefly describe the method we have used to calculate molecular dynamic polarizabilities [11,16,17,20,32,33,41] since it follows the work of Delley [31] and Görling et al. [11].

Since numerical basis functions are used to expand the Kohn–Sham orbitals, it is convenient to calculate the induced density and effective potentials on a real space molecular grid, \vec{r}_i , using the time-dependent Kohn–Sham density functional formalism [17,21,22, 42]. The Fourier component $\delta\rho(\vec{r}_i, \omega)$ of the induced density with the Fourier component of a time-dependent perturbation potential, $\delta v_{\text{ext}}(\vec{r}_i, \omega)$, is determined by linear response as follows:

$$\delta\rho(\vec{r}_i, \omega) = \int d\vec{r}' X_{\text{KS}}(\vec{r}_i, \vec{r}'; \omega) \delta v_{\text{eff}}(\vec{r}', \omega), \quad (1)$$

where $\delta v_{\text{eff}}(\vec{r}', \omega)$ is an effective potential defined as:

$$\begin{aligned} \delta v_{\text{eff}}(\vec{r}_i, \omega) = & \delta v_{\text{ext}}(\vec{r}_i, \omega) + \int d\vec{r}' \frac{\delta\rho(\vec{r}', \omega)}{|\vec{r}_i - \vec{r}'|} \\ & + \frac{\delta v_{\text{xc}}^{\text{LDA}}([\rho]; \vec{r}_i)}{\delta\rho(\vec{r}_i)} \delta\rho(\vec{r}_i, \omega) \end{aligned} \quad (2)$$

In Eq. (2), the second term is an induced Coulomb potential and the third term is an induced exchange-correlation potential with the local density approximation (LDA). The induced potential for a generalized gradient approximation exchange-correlation functional has one more term associated with it, but in this contribution we present only results using LDA. From Eq. (2), an induced Coulomb potential $\delta V^e(\vec{r}, \omega)$ is satisfied with the Poisson equation for response density $\delta\rho(\vec{r}, \omega)$ as follows:

$$\nabla^2 \delta V^e(\vec{r}, \omega) = -4\pi \delta\rho(\vec{r}, \omega)$$

In Eq. (1) the response function $X_{\text{KS}}(\vec{r}, \vec{r}', \omega)$ is given by,

$$\begin{aligned} X_{\text{KS}}(\vec{r}, \vec{r}', \omega) = & \sum_i^{\text{o.c.}} n_i \sum_a^{\text{vir}} \phi_i(\vec{r}) \phi_a(\vec{r}) \phi_a(\vec{r}') \phi_i(\vec{r}') \\ & \times \left[\frac{1}{\omega - \epsilon_a + \epsilon_i} - \frac{1}{\omega + \epsilon_a - \epsilon_i} \right], \end{aligned} \quad (3)$$

where n_i is the occupation number, $\phi_i(\vec{r})$ and $\phi_a(\vec{r})$ denote the spatial parts of the occupied and virtual KS orbitals with corresponding KS eigenvalues ϵ_i and ϵ_a ,

respectively. Here, we assume that KS orbitals to be real. The response density $\delta\rho(\vec{r}, \omega)$ is coupled through the induced Coulomb and exchange-correlation potentials, and is evaluated with a self-consistent-field procedure when complete knowledge of KS orbitals and eigenvalues are available. Finally, if $\delta v_{\text{ext}}(\vec{r}, \omega)$ is replaced by the x_j component of the dipole operator, the $\alpha_{ij}(\omega)$ component of the polarizability tensor is determined from the following integral:

$$\alpha_{ij}(\omega) = - \int d\vec{r} x_i \delta\rho^j(\vec{r}, \omega) \quad (4)$$

where $\delta\rho^j(\vec{r}, \omega)$ represents the response density due to the j th component of the dipole field with frequency ω .

The molecular isotropic polarizability, $\alpha(\omega)$, is defined as the mean value of three diagonal elements of the polarizability tensor, i.e.

$$\alpha(\omega) = \frac{1}{3}(\alpha_{xx}(\omega) + \alpha_{yy}(\omega) + \alpha_{zz}(\omega)) \quad (5)$$

For axially symmetric molecules, the polarizability anisotropy is given by,

$$\Delta\alpha(\omega) = \alpha_{zz}(\omega) - \alpha_{xx}(\omega) \quad (6)$$

More generally, for any polyatomic molecules, it is defined as:

$$\Delta\alpha(\omega)^2 = \frac{1}{2} \left[(\alpha_{xx}(\omega) - \alpha_{yy}(\omega))^2 + (\alpha_{xx}(\omega) - \alpha_{zz}(\omega))^2 + (\alpha_{yy}(\omega) - \alpha_{zz}(\omega))^2 \right] \quad (7)$$

The isotropic Cauchy coefficients, $S(-4)$, also known as the dipole oscillator strength sums, have been determined by calculating the quadratic regression constants of the following second-order frequency dependent approximation:

$$\alpha(\omega) = \alpha(0) + S(-4)\omega^2 \quad (8)$$

at several low frequencies. Frequency points were determined by the following relation:

$$f(i) = 0.95 \times \epsilon_{\text{HOMO-LUMO}} \frac{i}{N_{\text{sample}}} \quad (9)$$

where $\epsilon_{\text{HOMO-LUMO}}$ is the HOMO–LUMO gap and N_{sample} the number of frequency points. The factor of 0.95 is used to avoid the singularity in Eq. (3). For calculations of the water chains, as the number of

water molecules increases, the HOMO–LUMO gap decreases. Thus, the high frequency points were not stable due to the singularity in the linear response function (Eq. (3)). As a result, for all of the water chain calculations, the quadratic regression constants of the Cauchy coefficients were determined using the first five frequency points, only.

All calculations were carried out with the F95 numerical DFT package [43]. The KS orbitals are expanded in terms of numerical atomic basis functions [31] $\chi_\alpha(\vec{r} - \vec{a})$, which are given numerically as tabulated values on an atomic spherical-polar mesh centered at \vec{a} . The angular portion of each atomic orbital is real solid harmonics $C_m^l(\vec{r} - \vec{a})$ and radial one $R(\|\vec{r} - \vec{a}\|)$, obtained with the solution of atomic Kohn–Sham equations, is stored as set of cubic spline coefficients. The method to generate the numerical atomic basis sets that we have used is similar to the method developed by Delley [31,37–40]. We describe the procedure briefly. A minimal basis set is generated from an exact spherical DFT calculations on the neutral atom. Additional polarization and diffuse functions are generated from DFT calculations of ions, excited-state atoms and hydrogenic orbital calculations. Using a standard double numerical basis set with polarization functions available in Dmol, Guan et al. have calculated static molecular polarizabilities within the finite field approximation [35]. The polarizabilities calculated for small molecules were in good agreement with experimental values. Later, Dickson and Becke calculated molecular polarizabilities using their basis-free method [44] within the finite field approximation, and compared them to the results of Guan et al. [35]. The results were in excellent agreement except for the calculated hyperpolarizabilities. It is known that molecular polarizabilities can be sensitive to basis set effects. As a result, for this work we have included an extensive augmentation set to our basis. Following Delley's procedure to generate numerical basis functions [31], we have used a larger group of hydrogenic calculations. For hydrogen, a basis set with a 4s 3p 2d 2f structure has been employed. This compares to the 2s 1p numeric basis set used by Guan and co-workers. For first row elements (C, N, O) basis set with a 8s 7p 5d 5f structure

Table 1
Static dipole polarizabilities in atomic units

Molecule	Property	Numerical basis (this work)	Basis set free ^a	d-aug-ccpVTZ basis set ^b	Expt. ^c
H ₂ O	$\bar{\alpha}$	10.52	10.60	10.60	9.64
	$ \Delta\alpha $	0.16	0.02	0.04	0.67
	α_{xx}	10.38	10.59		
	α_{yy}	10.64	10.61		
	α_{zz}	10.55	10.59		
N ₂	$\bar{\alpha}$	12.19	12.30	12.23	11.74
	$ \Delta\alpha $	4.76	4.63	4.59	4.59
	α_{xx}	10.61	10.73		
	α_{zz}	15.36	15.43		
CO	$\bar{\alpha}$	13.68	13.70		13.08
	$ \Delta\alpha $	3.30	3.30		3.6
	α_{xx}	12.58	12.61		
	α_{zz}	15.88	15.88		
NH ₃	$\bar{\alpha}$	15.40	15.54	15.55	14.56
	$ \Delta\alpha $	2.72	2.90	2.88	1.94
	α_{xx}	14.49	14.59		
	α_{zz}	17.21	17.46		
CH ₄	α_{xx}	17.37	17.69	17.98	17.27

^a Results of Dickson and Becke in Ref. 44.

^b Results of Van Caillie and Amos [46].

^c Results of Meath and co-workers [52–57].

was used in comparison to a 3s 2p 1d basis set, which was used by Guan et al. [35].

All calculations have been performed using the LDA in the parameterization of Vosko et al. [45]. For the majority of the molecules considered, the geometries have been taken from the work of Sekino and Bartlett [3], as well as Van Caillie and Amos [46]. The geometries of CH₄, C₂H₂ and C₂H₆ are given in Ref. 46 whereas the geometries of H₂O, CO, CO₂, N₂ and NH₃ are given in Ref. 3 and references therein. Geometries of the water chains were obtained by geometry optimization at the LDA level imposing a C_{2v} symmetry constraint. To visualize induced density components $\delta\rho_{xx}(\vec{r}_i, \omega = 0)$, $\delta\rho_{zz}(\vec{r}_i, \omega = 0)$, and the HOMO and LUMO orbitals, a 10 × 10 × 40 rectangle box was used with a 0.3 a.u. grid mesh.

3. Results and discussion

This work follows two recent studies of molecular polarizabilities determined with DFT at the LDA level. Using a basis set free method, Dickson and Becke [44]

determined static isotropic and anisotropic polarizabilities of some small molecules. Van Caillie and Amos [46] have determined both static and dynamic molecular polarizabilities using two Gaussian basis sets. The first basis set is due to Sadlej [47,48] has a 3s 2p structure for hydrogen and a 5s 3p 2d structure for C, N and O and can be characterized as medium sized. The second basis set used was the doubly augmented correlation consistent basis (d-aug-ccpVTZ) of Dunning [49,50] which has a 5s 4p 4d structure for H and a 6s 5p 4d 3f structure for C, N and O. Compared to the Sadlej basis set, the d-aug-ccpVTZ basis set has more high angular momentum and diffuse functions. The numerical basis set we have used in the present calculations has a 4s 3p 2d 2f structure for H and a 8s 7p 5d 5f structure for C, N and O. Thus, this basis has even more diffuse high angular momentum functions. The available experimental data are also listed for ease of comparison, which are given by Spackman [51]. The Cauchy moments are given in Table 2 together with the results from Amos and co-worker, and the available experimental data largely from the work of Meath and co-workers [52–57].

Table 2
 $S(-4)$ Cauchy coefficients in atomic units

Molecule	Property	Numerical basis (this work)	d-aug-ccpVTZ basis ^a	Expt. ^b
H ₂ O	$\bar{S}(-4)$	50.11	48.91	35.42
	$ \Delta S(-4) $	29.88	32.50	
	$S(-4)_{xx}$	68.45		
	$S(-4)_{yy}$	34.20		
	$S(-4)_{zz}$	47.68		
N ₂	$\bar{S}(-4)$	34.57	34.25	30.11
	$ \Delta S(-4) $	18.71	17.53	
	$S(-4)_{xx}$	28.34		
	$S(-4)_{zz}$	47.05		
CO ₂	$\bar{S}(-4)$	52.54	52.39	
	$ \Delta S(-4) $	65.57	64.31	
	$S(-4)_{xx}$	30.69		
	$S(-4)_{zz}$	96.27		
NH ₃	$\bar{S}(-4)$	104.05	99.26	71.44
	$ \Delta S(-4) $	126.25	119.46	
	$S(-4)_{xx}$	61.97		
	$S(-4)_{zz}$	188.23		
CH ₄	$S(-4)_{xx}$	68.15	72.12	62.41
C ₂ H ₂	$\bar{S}(-4)$	140.23	130.96	113.5
	$ \Delta S(-4) $	78.15	70.58	
	$S(-4)_{xx}$	114.17		
	$S(-4)_{zz}$	192.32		
C ₂ H ₄	$\bar{S}(-4)$	179.57	166.71	143.5
	$ \Delta S(-4) $	115.39	114.13	
	$S(-4)_{xx}$	148.91		
	$S(-4)_{yy}$	104.49		
	$S(-4)_{zz}$	285.30		
C ₂ H ₆	$\bar{S}(-4)$	116.88	121.04	108.1
	$ \Delta S(-4) $	31.52	35.43	
	$S(-4)_{xx}$	106.37		
	$S(-4)_{zz}$	137.90		

^a Results of Van Caillie and Amos [46].

^b Results of Meath and co-workers [52–57].

3.1. Static and dynamic polarizabilities

The calculated static polarizabilities and their anisotropies are listed in Table 1 along with the basis-set free results of Dickson and Becke [44] and the results of Amos and co-worker [46] computed with the d-aug-ccpVTZ Gaussian basis set. The available experimental data given by Spackman [51] is also listed. Several studies of molecular static polarizabilities with DFT at the LDA and GGA level have been made [24,35,58,59]. Most employed the

finite-field approach, fewer studies have used the coupled-perturbed scheme as in the present study. A comparison of our results with previous DFT calculations of the static polarizability are of interest as a means of validating our implementation of the coupled-perturbed scheme.

Our results are in excellent agreement with the previous LDA calculations for the admittedly small set of molecules we have tested. The static isotropic polarizabilities show an rms difference of 1.05 and 1.81% compared to the basis free and d-aug-ccpVTZ

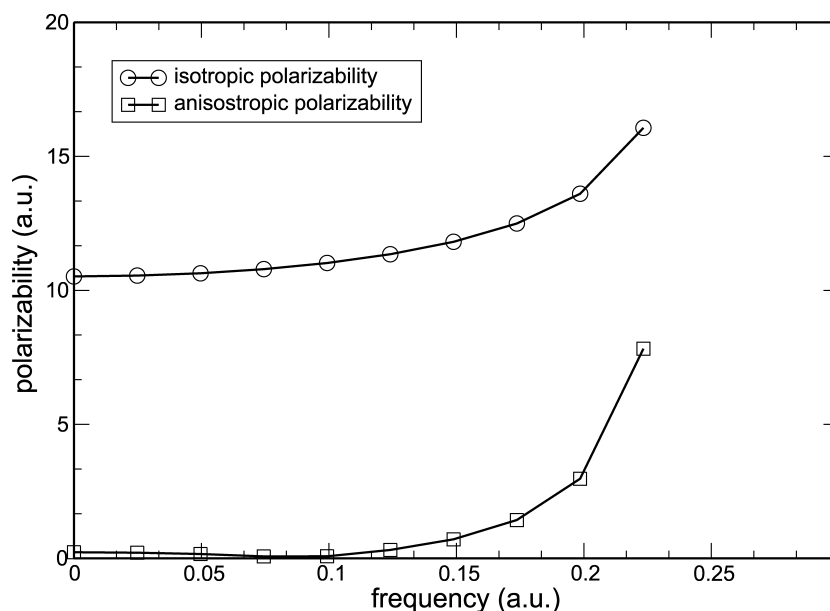


Fig. 1. Frequency dependence of the isotropic and anisotropic polarizability of a single water molecule calculated with time-dependent DFT at the LDA level.

results, respectively. Our results are in closer agreement with the basis set free results. This might be expected since we have used a larger basis set than Van Caillie and Amos and the results of Dickson and Becke can be considered at the basis set limit. Compared to experimental values, the LDA results generally overestimate the static isotropic polarizabilities. The LDA results compared with experimental values and other ab initio and DFT results has been previously discussed [46]. The polarizability anisotropies, $|\Delta\alpha|$, are also in excellent agreement with earlier calculations with the exception of water. For water we calculate a value of $|\Delta\alpha| = 0.16$ a.u., while the basis free and d-aug-ccpVTZ results give values of 0.02 and 0.04 a.u., respectively. The experimental result which includes vibrational and dispersion effects has been determined to be 0.67 [60]. Other calculations have also shown anomalous values of the anisotropic polarizability of water [44,58]. At the LDA level, Guan et al. predict $|\Delta\alpha| = 0.43$ with their best basis set, while Sim et al. report a value of 0.328 a.u. It is unclear why there are such large discrepancies in the reported values of the polarizability anisotropy for water. The results of Van Caillie and Amos suggest that it might be basis set dependent. Using the d-aug-ccpVTZ basis they determine $|\Delta\alpha| =$

0.04 while with the smaller Sadlej basis set this changes to 0.24 a.u. at the LDA level.

Although reports of static molecular polarizabilities determined at the DFT level are numerous, reports of dynamic molecular polarizabilities at the DFT level have been limited [11,14,20,25,26,46,59]. Reports of the Cauchy coefficients are particularly scarce [11,46,61]. One purpose of this contribution is to compare our results of the $S(-4)$ Cauchy coefficients and their anisotropies, $\Delta S(-4)$, to those of Van Caillie and Amos. The primary difference in our approach is the use of a rather large numerical basis set compared to the Gaussian basis set used by Van Caillie and Amos.

For a small set of molecules, the values of the $S(-4)$ Cauchy coefficients as well as their anisotropies are given in Table 2, along with the results of Van Caillie and Amos. The available experimental data due to the work of Meath [52–56,62] are also given. Our results for the isotropic $S(-4)$ Cauchy coefficient are in good agreement with the results of Van Caillie and Amos, however, there is more deviation than in the static polarizabilities. The rms deviation in the $S(-4)$ Cauchy coefficient was found to be 4.8% which compares to 1.8% for the static isotropic polarizabilities. The LDA results, both ours

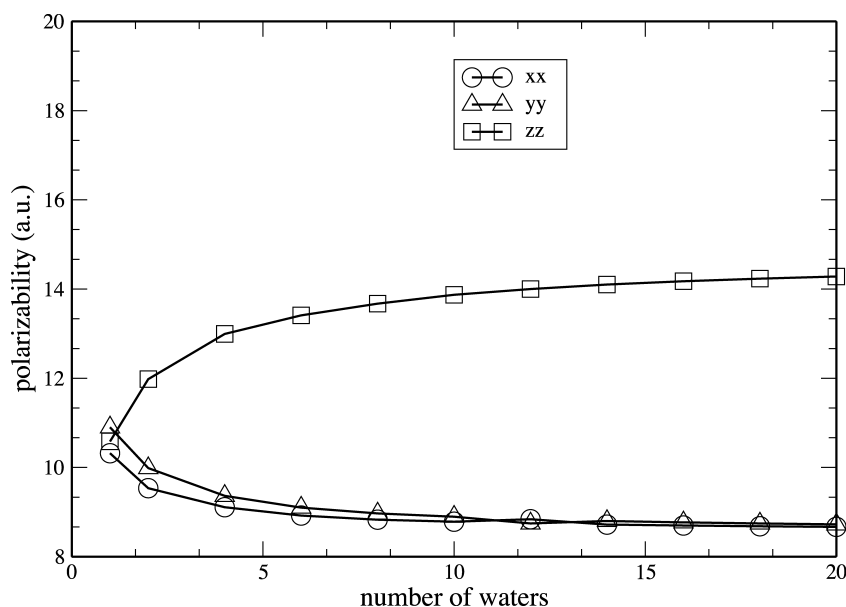


Fig. 2. Calculated static polarizabilities per water molecule as a function of the size of the water chain.

and those of Van Caillie and Amos, generally overestimate the experimental $S(-4)$ Cauchy coefficients. Our results for the anisotropy of the $S(-4)$ Cauchy coefficient are also in reasonable agreement with the results of Van Caillie and Amos with an rms deviation of 7.44%.

The largest deviations between our results and those of Van Caillie and Amos for the isotropic $S(-4)$ Cauchy coefficients occur for C_2H_2 and C_2H_4 . For acetylene, C_2H_2 , Van Caillie and Amos suggest that the results might be sensitive to the basis set used since they obtained a value of 130.96 a.u. using the d-aug-ccpVTZ basis and a value of 138.28 a.u. using the smaller Sadlej basis set. Interestingly, our calculated result of 140.23 a.u. using a large numerical basis for acetylene compares more favorably to the smaller Sadlej basis set result. To examine the convergence of the numerical basis set, we have calculated the Cauchy coefficient for acetylene using smaller basis with a 8s 7p 5d structure for carbon and a 3s 2p 1d structure for hydrogen. We find a difference of only 0.01 a.u. in the computed values suggesting that our numerical basis set is well converged. Both the $S(-4)$ Cauchy coefficient and its anisotropy for acetylene show the largest deviations. However, for ethene the discrepancy is only large for the isotropic value with

the anisotropy, $\Delta S(-4)$, being in excellent agreement. The origin of the inconsistencies between our numerical basis set calculations and the results of Van Caillie and Amos is unknown. One possible explanation aside from the differing basis sets has its origin in the frequency window used for the quadratic fit of the $S(-4)$ coefficient. In our calculations we have used a frequency window that is at least twice as large as that used by Van Caillie and Amos. Specifically, they used a frequency window of 0.00–0.089 a.u. whereas we used a window of 0.00–0.2 a.u. or greater.

It is worth commenting on the dynamical isotropic and anisotropic polarizabilities $\bar{\alpha}(\omega)$ and $\Delta\alpha(\omega)$, of water at the LDA level. We have already mentioned that the anisotropy of the static polarizability of water is small and that there are notable discrepancies in the reported values at the LDA level. Shown in Fig. 1 is the frequency dependence of $\bar{\alpha}(\omega)$ and $\Delta\alpha(\omega)$ over the range for which the Cauchy expansion was performed. As the frequency is increased from zero, the anisotropy decreases and is close to zero at a frequency of about 0.1 a.u. At this point it increases again. High level coupled cluster singles and doubles linear response function method (CCSDLR) calculations of Dalskov and Sauer [63] also reproduce this.

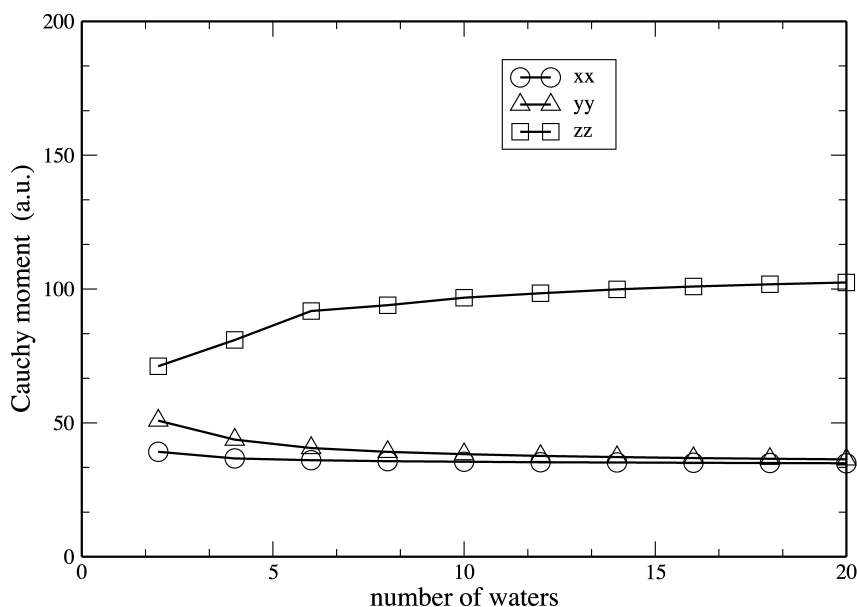


Fig. 3. Calculated $S(-4)$ Cauchy coefficient per water molecule as a function of the size of the water chain.

3.2. Polarizabilities of water chains and scaling of the calculations

In Section 3.1 we have examined the static and dynamic polarizabilities of small molecules with numerical atomic basis sets. Accurate methods to calculate dynamic polarizabilities and hyperpolarizabilities of large molecular systems or infinite periodic systems [5,6,64–66] is of increasing interest due to applications in the field of non-linear optical materials. To examine the efficiency of our approach for treating large systems, we have calculated the static and dynamic polarizabilities of a linear chain of bifurcated water molecules ranging from 1 to 20 molecules in length.

Figs. 2 and 3 give the static polarizabilities per molecule and the $S(-4)$ Cauchy coefficient per molecule, respectively, of the bifurcated water chains. The z -direction is defined as lying along the axis of the chain (left to right in Fig. 4). The polarization along the chain in the z -direction, increases as more molecules are added, whereas it diminishes for the components perpendicular to the chain axis. Convergence occurs rapidly, at which point the polarizability of the system is a linear function of the number of water molecules. This suggests that there is very little charge transfer between the molecules. Shown in Fig.

4(a) and (b) are isosurface plots of the HOMO and LUMO Kohn–Sham orbitals, respectively, for the 12 molecule water chain. The HOMO and LUMO orbitals are highly localized at opposite ends of the chain, thus, suggesting that charge transfer is inhibited. Fig. 4(c) shows the induced density when the applied field is parallel to the axis of the chain. The induced density does not show a build-up at the ends of the water chain, again suggesting little charge transfer.

In order to perform practical simulations of large molecular systems, it is of interest to understand how the computational effort of our approach scales with the size of the system. Shown in Fig. 5 are the total CPU times required for the polarizability calculations of water chains of varying size. Up to the twenty water molecule chain tested, the calculation scales as $O(N^{1.8})$. A detailed discussion using numerical basis sets has been provided by Delley [31]. For response property calculations, the most time consuming portion of the calculation is the evaluation of the matrix of effective potentials over basis functions and induced densities. This is done numerically over a real space molecular grid. The time required for this component of the calculation is shown in Fig. 5. The evaluation of the matrix element of the effective potential consists of integrating $\delta v_{\text{eff}}(\vec{r}', \omega)$ in Eq. (2).

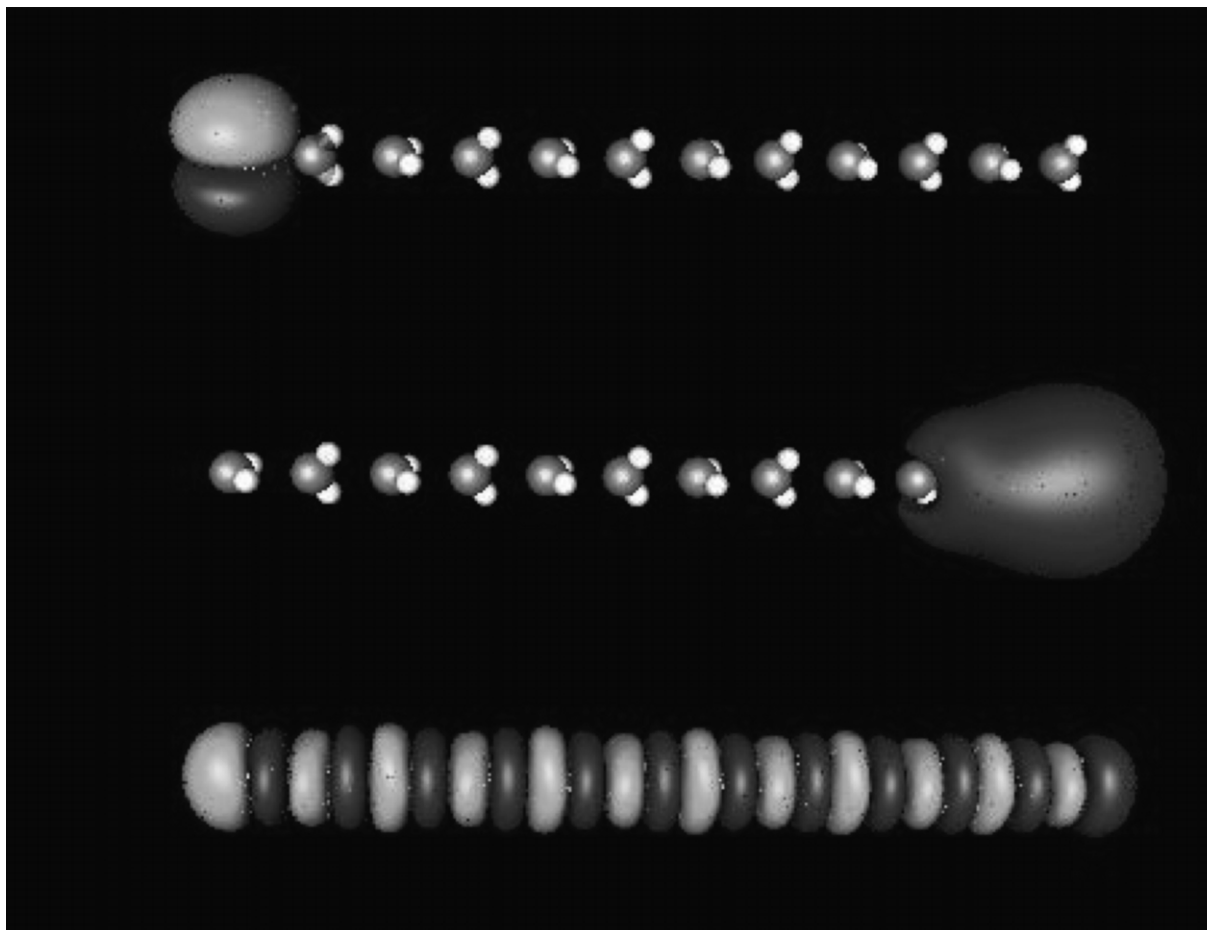


Fig. 4. Isosurface plots at 0.003 a.u. of the HOMO (a) and LUMO (b) orbitals of the 12 molecule water chain (c) is an isosurface plot of the total induced density when the applied field lies along the chain of the water molecules. Dark isosurface is an increased density, while the light surface is a diminished density.

In evaluating the effective potentials over molecular grids, there are three terms from Eq. (2). The evaluation of the first and third terms scales as $O(N)$. This is because with the numerical integration procedure the number of operations is proportional to the number of grid points, which is proportional to the number of atoms contained in a molecule. To evaluate the second term in Eq. (2), the induced Coulomb potential, there are corresponding Poisson equations to be solved. In our calculations, we used the partitioning approach of Delley [31], in which induced molecular densities are first partitioned into induced atomic densities with a rapidly convergent multipolar expansion. Then, these atomic densities are

decomposed into multipolar components using the so-called projection methods of Delley. However, instead of using spherical harmonics, we utilized real solid harmonics in the density projections. There are two reasons for this. First, the angular parts of our numerical basis functions are expanded in terms of real solid harmonics. Second, the multipolar components are simply given by the products of multipolar strengths and solid harmonics. The corresponding Coulomb potential components are calculated using Green's function of the Laplacian. Up to this point the determination of the induced Coulomb potential scales as $O(N)$. Finally, the total induced Coulomb potential is obtained with

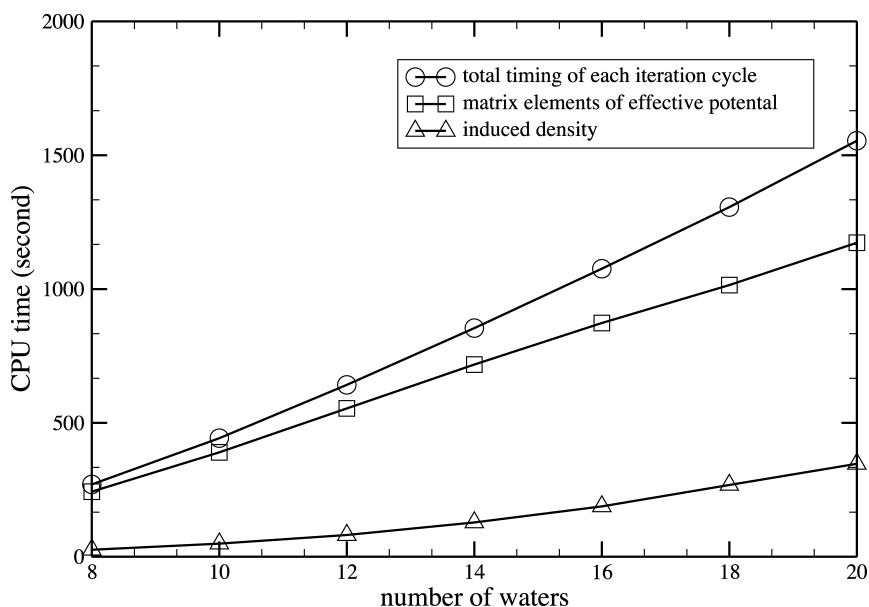


Fig. 5. CPU timings for the polarizability calculations the water chain as a function of the size of the chain. Shown are the total time, and the times required to evaluate the matrix elements of the effective potential as well as the response density.

summations of these multipolar components over the atoms and the angular momenta. This step scales as $O(N^2)$ [31]. Although the calculation of the induced Coulomb potential formally scales as $O(N^2)$, this is only a small portion of the whole computational effort required to evaluate the matrix elements. So, in the range tested the evaluation of the matrix elements of the effective potential scales as $O(N^{1.4})$.

The determination of the response densities (Eq. (1)), is the next most time consuming component of the overall calculation. The timings of this component is also shown in Fig. 5. Since summation over occupied orbitals is required here, the determination of the response densities scales beyond $O(N)$. However, as can be seen in Fig. 5, the time required for this component is less than half of that required for the effective potential matrix elements.

4. Conclusions

The use of atomic numerical basis functions within the TDDFT framework provides an efficient approach for determining static and dynamic polarizabilities that give results that are in excellent agreement with basis set free and more

common Gaussian basis sets. Static polarizabilities and their anisotropies of small first row element compounds agree well with previous LDA results. The only exception is the anisotropic polarizability of water for which a number of groups have reported inconsistencies. DFT reports of $S(-4)$ Cauchy coefficients and dynamic polarizabilities are rare, but our calculations agree well with past results of Van Caillie and Amos for a set of small molecules. However, the agreement between our results and those of Van Caillie and Amos is not as good as the agreement observed with the static polarizabilities. This suggests that the dynamic polarizabilities calculated with DFT may be more basis set dependent or that the calculations are sensitive to the size of the frequency window used to determine the Cauchy coefficients.

Using a linear chain of water molecules ranging between 1 and 20 molecules in size, we have determined that the calculation of the dynamic polarizability with our implementation, scales as $O(N^{1.8})$. This shows that the straightforward evaluation of induced densities and effective potentials over molecular grids with numerical basis functions is an efficient approach for determining response properties and therefore has

promise for the accurate determination of these properties for large molecular systems. Although the results shown in this paper are calculated with the local spin density approximation, the scaling of the calculation will not be different when using the generalized gradient approximation. The method also allows for easy parallelization, which we are planning to address in the near future.

Acknowledgments

We would like to acknowledge NSERC of Canada and SHARCnet at the University of Western Ontario for financial support. DY is grateful for financial support provided by the National Institutes of Health (Grant 1R01-GM62248-01A1), and the Donors of The Petroleum Research Fund, administered by the American Chemical Society, and the Minnesota Supercomputing Institute through a research scholar award (AH). Computational resources were provided by the Minnesota Supercomputing Institute.

References

- [1] W.J. Meath, *At. Mol. Phys. Quantum Opt., Proc. Phys. Summer Sch.* 5 (1992) 157.
- [2] H. Sekino, R.J. Bartlett, *ACS Symp. Ser.* 628 (1996) 79.
- [3] H. Sekino, R.J. Bartlett, *J. Chem. Phys.* 98 (1993) 3022.
- [4] H. Sekino, R.J. Bartlett, *J. Chem. Phys.* 85 (1986) 976.
- [5] B. Kirtman, F.L. Gu, D.M. Bishop, *J. Chem. Phys.* 113 (2000) 1294.
- [6] D.M. Bishop, J.M. Luis, B. Kirtman, *J. Chem. Phys.* 108 (1998) 10013.
- [7] J. Oddershede, N.E. Grunener, G.H.F. Dierchsen, *Chem. Phys.* 97 (1985) 303.
- [8] H.F. Hamerka, E.N. Svendsen, *Int. J. Quantum Chem., Quantum Chem. Symp.* 18 (1984) 519.
- [9] M. Hasan, S.-J. Kim, J.L. Toto, B. Kirtman, *J. Chem. Phys.* 105 (1996) 186.
- [10] P.W. Langhoff, S.T. Epstein, M. Karplus, *Rev. Mod. Phys.* 44 (1972) 620.
- [11] A. Gorling, H.H. Heinze, S.P. Ruzankin, M. Staufer, N. Rosch, *J. Chem. Phys.* 110 (1999) 2785.
- [12] R. van Leeuwen, *Phys. Rev. Lett.* 80 (1998) 1280.
- [13] S. Ivanov, R. Lopez-Boada, A. Gorling, M. Levy, *J. Chem. Phys.* 109 (1998) 6280.
- [14] V.P. Osinga, S.J.A. van Gisbergen, J.G. Snijders, E.J. Baerends, *J. Chem. Phys.* 106 (1997) 5091.
- [15] D.A. Dixon, N. Matsuzawa, *J. Phys. Chem.* 98 (1994) 3967.
- [16] A. Zangwill, *J. Chem. Phys.* 78 (1983) 5926.
- [17] E.K.U. Gross, J.F. Dobson, M. Petersilka, *Top. Curr. Chem.* 181 (1996) 81.
- [18] N. Matsuzawa, M. Ata, D.A. Dixon, *J. Phys. Chem.* 99 (1995) 7698.
- [19] N. Matsuzawa, D.A. Dixon, *J. Phys. Chem.* 98 (1994) 2545.
- [20] S.J.A. van Gisbergen, J.G. Snijders, E.J. Baerends, *J. Chem. Phys.* 103 (1995) 9347.
- [21] A. Zangwill, P. Soven, *Phys. Rev. A* 21 (1980) 1561.
- [22] E. Runge, E.K.U. Gross, *Phys. Rev. Lett.* 52 (1984) 997.
- [23] S.M. Colwell, N.C. Handy, A.M. Lee, *Phys. Rev. A: At. Mol., Opt. Phys.* 53 (1996) 1316.
- [24] S.M. Colwell, C.W. Murray, N.C. Handy, R.D. Amos, *Chem. Phys. Lett.* 210 (1993) 261.
- [25] A. Gorling, *Int. J. Quantum Chem.* 69 (1998) 265.
- [26] S.J.A. van Gisbergen, V.P. Osinga, O.V. Gritsenko, R. van Leeuwen, J.G. Snijders, E.J. Baerends, *J. Chem. Phys.* 105 (1996) 3142.
- [27] D.E. Beck, *Phys. Rev. B: Condens. Matter* 30 (1984) 6935.
- [28] M. Petersilka, U.J. Gossmann, E.K.U. Gross, *Phys. Rev. Lett.* 76 (1996) 1212.
- [29] H. Sekino, R.J. Bartlett, *Chem. Phys. Lett.* 234 (1995) 87.
- [30] H. Sekino, R.J. Bartlett, *Int. J. Quantum Chem., Quantum Chem. Symp.* 18 (1984) 255.
- [31] B. Delley, *J. Chem. Phys.* 92 (1990) 508.
- [32] A.M. Lee, S.M. Colwell, *J. Chem. Phys.* 101 (1994) 9704.
- [33] M.E. Casida, in: D.P. Chong (Ed.), *Recent Advances in Computational Chemistry*, World Scientific, Singapore, 1995, pp. 155–192.
- [34] M.E. Casida, *Book of Abstracts, 213th ACS National Meeting, San Francisco, COMP, April 13–17, 1997.*
- [35] J. Guan, P. Duffy, J.T. Carter, D.P. Chong, K.C. Casida, M.E. Casida, M. Wrinn, *J. Chem. Phys.* 98 (1993) 4753.
- [36] A. Hu, K. Range, D.M. York, in preparation.
- [37] B. Delley, in: J.K. Labanowski, J.W. Andzelm (Eds.), *Density Functional Methods in Chemistry*, Springer-Verlag, New York, 1991, pp. 101–107.
- [38] B. Delley, *J. Chem. Phys.* 94 (1991) 7245.
- [39] B. Delley, *J. Chem. Phys.* 113 (2000) 7756.
- [40] B. Delley, *Comput. Mater. Sci.* 17 (2000) 122.
- [41] M.J. Stott, E. Zaremba, *Phys. Rev. A* 21 (1980) 12.
- [42] G.D. Mahan, *Phys. Rev. A* 22 (1980) 1780.
- [43] A. Hu, K. Range, D.M. York, NUDFT: A parallel linear-scaling numerical density-functional program, Version 1.0, developed at the University of Minnesota (<http://riesling.chem.umn.edu>).
- [44] R.M. Dickson, A.D. Becke, *J. Phys. Chem.* 100 (1996) 16105.
- [45] S.H. Vosko, L. Wilk, M. Nusair, *Can. J. Phys.* 58 (1980) 1200.
- [46] C.V. Caillie, R.D. Amos, *Chem. Phys. Lett.* 291 (1998) 71.
- [47] A.J. Sadlej, *Collect. Czech. Chem. Commun.* 53 (1988) 1995.
- [48] A.J. Sadlej, *Theor. Chim. Acta* 79 (1991) 123.
- [49] D.E. Woon, T.H. Dunning Jr., *J. Chem. Phys.* 98 (1993) 1358.
- [50] D.E. Woon, T.H. Dunning Jr., *J. Chem. Phys.* 100 (1994) 2975.
- [51] M.A. Spackman, *J. Chem. Phys.* 94 (1991) 1288.
- [52] A. Kumar, W.J. Meath, *Can. J. Chem.* 63 (1985) 1616.
- [53] A. Kumar, W.J. Meath, *Can. J. Phys.* 63 (1985) 417.
- [54] B.L. Jhanwar, W.J. Meath, *J. Chem. Phys.* 67 (1982) 185.

- [55] B.L. Jhanwar, W.J. Meath, *Can. J. Phys.* 61 (1983) 1027.
- [56] G.D. Zeiss, W.J. Meath, J.C.F. MacDonald, D.J. Dawson, *Can. J. Phys.* 55 (1977) 2080.
- [57] G.D. Zeiss, W.J. Meath, *Mol. Phys.* 33 (1977) 1155.
- [58] P. Calaminici, K. Jug, A.M. Koster, *J. Chem. Phys.* 109 (1998) 7756.
- [59] S.A.C. McDowell, R.D. Amos, N.C. Handy, *Chem. Phys. Lett.* 235 (1995) 1.
- [60] W.F. Murphy, *J. Chem. Phys.* 67 (1977) 5877.
- [61] C. Jamorski, M.E. Casida, D.R. Salahub, *J. Chem. Phys.* 104 (1996) 5134.
- [62] R.J. Pazur, A. Kumar, R.A. Thuraisingham, W.J. Meath, *Can. J. Chem.* 66 (1988) 615.
- [63] E.K. Dalskov, S.P.A. Sauer, *J. Phys. Chem. A* 102 (1998) 5269.
- [64] D.M. Bishop, F.L. Gu, B. Kirtman, *J. Chem. Phys.* 114 (2001) 7633.
- [65] B. Kirtman, Book of Abstracts, 218th ACS National Meeting, New Orleans, COMP, August 22–26, 1999.
- [66] B. Kirtman, J.M. Luis, D.M. Bishop, *J. Chem. Phys.* 108 (1998) 10008.